Temperature Dependence of O_2 ($^1\Delta$) + O_2 ($^1\Delta$) and I($^2P_{1/2}$) + O_2 ($^1\Delta$) Energy Pooling

Temperature Dependence of O_2 (1 Delta) + O_2 (1 Delta) and I(2P sub 1/2) + O_2 (1 Delta) Energy Pooling.

R. F. HEIDNER III, C. E. GARDNER, G. I. SEGAL,
and T. M. EL-SAYED
Aerophysics Laboratory
Laboratory Operations
The Aerospace Corporation
El Segundo, Calif. 90245

and

J. V. V. KASPER
Department of Chemistry
University of California
Los Angeles, Calif. 90024

Raymond F. /Heidner, III
Carrel E. /Gardner
G. I. /Segal
T. M. /El-Sayed
J. V. V. /Kasper

1 September 1981

Technical rept.,

TR-0081(6940-01)-2

F04701-80-C-0081

DTIC
ELECTED
OCT 19 1981
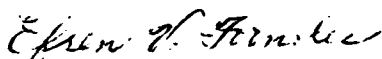
D

10

This report was submitted by The Aerospace Corporation, El Segundo, CA 90245, under Contract No. F04701-80-C-0081 with the Space Division, Deputy for Technology, P.O. Box 92960, Worldway Postal Center, Los Angeles, CA 90009. It was reviewed and approved for The Aerospace Corporation by W. P. Thompson, Jr., Director, Aerophysics Laboratory. Lieutenant Efren Fornoles, SD/YLXT, was the projet officer for Mission-Oriented Investigation and Experimentation (MOIE) Programs.
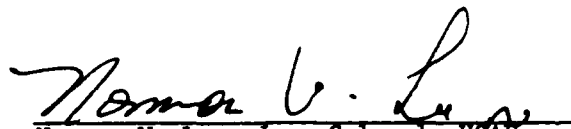
This report has been reviewed by the Public Affairs Office (PAS) and is releasable to the National Technical Information Service (NTIS). At NTIS, it will be available to the general public, including foreign nations.

This technical report has been reviewed and is approved for publication. Publication of this report does not constitute Air Force approval of the report's findings or conclusions. It is published only for the exchange and stimulation of ideas.

Effen V. Fornoles, 2nd Lt, USAF
Project Officer

Florian P. Meinhardt, Lt. Col., USAF
Director of Advanced Space
Development

FOR THE COMMANDER

Norman W. Lee, Jr., Colonel, USAF
Deputy for Technology

REPORT DOCUMENTATION PAGE		READ INSTRUCTIONS BEFORE COMPLETING FORM
1. REPORT NUMBER SD-TR-81-65	2. GOVT ACCESSION NO. AD-4105817	3. RECIPIENT'S CATALOG NUMBER
4. TITLE (and Subtitle) TEMPERATURE DEPENDENCE OF $O_2(^1\Delta) + O_2(^1\Delta)$ AND $I(^2P_{1/2}) + O_2(^1\Delta)$ ENERGY POOLING		5. TYPE OF REPORT & PERIOD COVERED
		6. PERFORMING ORG. REPORT NUMBER TR-0081(6940-01)-2
7. AUTHOR(s) Raymond F. Heidner III, Carrol E. Gardner, G. I. Segal, T. M. El-Sayed, and J. V. V. Kasper		8. CONTRACT OR GRANT NUMBER(s) F04701-80-C-0081
9. PERFORMING ORGANIZATION NAME AND ADDRESS The Aerospace Corporation El Segundo, Calif. 90245		10. PROGRAM ELEMENT, PROJECT, TASK AREA & WORK UNIT NUMBERS
11. CONTROLLING OFFICE NAME AND ADDRESS Space Division Air Force Systems Command Los Angeles, Calif. 90009		12. REPORT DATE 1 September 1981
		13. NUMBER OF PAGES 38
14. MONITORING AGENCY NAME & ADDRESS(if different from Controlling Office)		15. SECURITY CLASS. (of this report) Unclassified
		15a. DECLASSIFICATION/DOWNGRADING SCHEDULE

16. DISTRIBUTION STATEMENT (of this Report)

Approved for public release; distribution unlimited

17. DISTRIBUTION STATEMENT (of the abstract entered in Block 20, if different from Report)

18. SUPPLEMENTARY NOTES

19. KEY WORDS (Continue on reverse side if necessary and identify by block number)

Energy Pooling
Excited Oxygen
Iodine Laser
Kinetic Flow Tube

20. ABSTRACT (Continue on reverse side if necessary and identify by block number)

The electronic-energy pooling reactions forming $O_2(^1\Sigma)$ are of critical importance to the overall mechanism of the $O_2(^1\Delta)$ - I atom transfer laser. In this study, we report temperature-dependent rate coefficient data for $O_2(^1\Delta) + O_2(^1\Delta) \xrightarrow{k_2} O_2(^1\Sigma) + O_2(^3\Sigma)$ and $O_2(^1\Delta) + I(^2P_{1/2}) \xrightarrow{k_3} O_2(^1\Sigma) + I$. These data were obtained using a temperature-controlled kinetic flow tube equipped with computer-controlled spectroscopic diagnostics. The fundamental data

DD FORM 1473
(FACSIMILE)

19. KEY WORDS (*Continued*)

20. ABSTRACT (*Continued*)

reported are $k_2(T)/k_2(295) = (3.5 \pm 1.5) \exp(-780/RT)$ and $k_3(T)/k_2(T) = (5.5 \pm 1.0) \times 10^3$. Both rate-coefficient ratios are reported for the temperature range $T = 259$ to 353 K. The results are compared with earlier measurements of these processes.

PREFACE

Accession For	
NTIS GRA&I	X
DTIC TAB	☐
Unannounced	☐
Justification	
By	
Distribution/	
Availability Codes	
Dist	Avail and/or Special

DTIC
ELECTE
SEP 10 1981

D

1

CONTENTS

FIGURES

TABLES

I. INTRODUCTION

A number of years ago, Arnold et al.[1] observed that several complex electronic-energy transfer processes occurred when I_2 was injected into a stream of electronically excited oxygen [$O_2(^1\Delta)$ and $O_2(^1\Sigma)$]. In more detailed studies of this kinetic system, Derwent and Thrush[2] suggested that one of these transfer processes, the rapid equilibration

$$O_2(^1\Delta) + I(^2P_{3/2}) \xrightarrow[k_{-1}]{k_1} O_2(^3\Sigma) + I(^2P_{1/2}) \qquad (1)$$
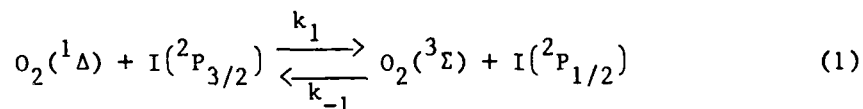
between near-resonant electronic states of the oxygen molecule and the iodine atom, could pump a continuous-wave iodine atom laser at 1.315 μm. The relevant electronic states of O_2, I_2, and I are shown in Figure 1. Recently, this suggestion was successfully implemented by McDermott et al.[3] shortly after related experiments had demonstrated gain on the I-atom transition.[4]

In the early kinetic studies, Derwent and Thrush[5-8] assigned a very important role to the energy-pooling reactions that produced $O_2(^1\Sigma)$:

$$O_2(^1\Delta) + O_2(^1\Delta) \xrightarrow{k_2} O_2(^1\Sigma) + O_2(^3\Sigma) \qquad (2)$$

$$O_2(^1\Delta) + I^* \xrightarrow{k_3} O_2(^1\Sigma) + I \qquad (3)$$
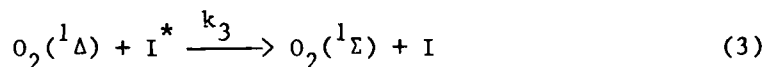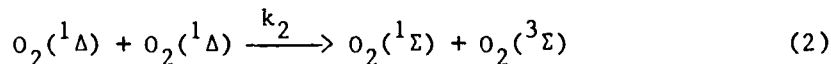
(In these equations and the text that follows, I and I^* refer to the $^2P_{3/2}$ and $^2P_{1/2}$ states of the iodine atom, respectively.) That role was the initiation and maintenance of I_2 dissociation by the electronic-energy transfer process

9
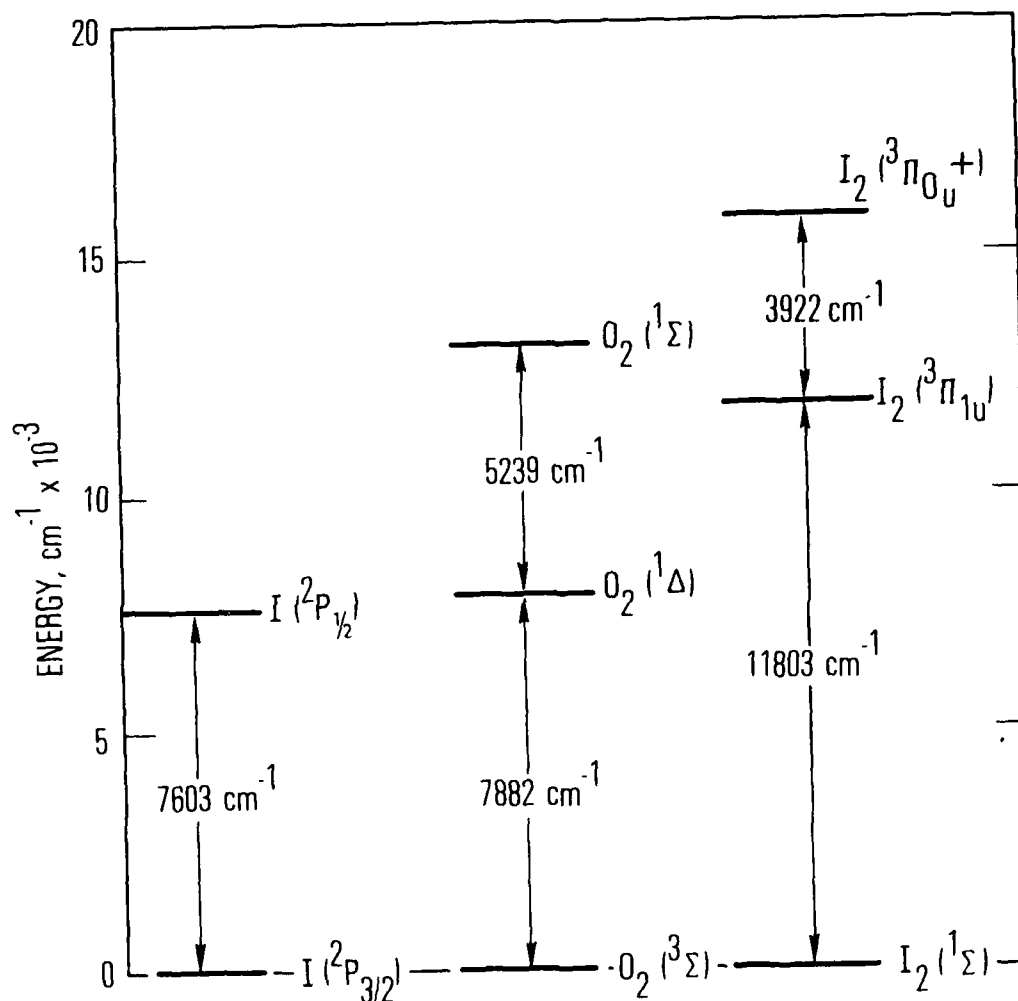
Figure 1. Low-Lying Electronic Energy Levels of the O_2 and I_2 Molecules and the I Atom

$$O_2(^1\Sigma) + I_2 \xrightarrow{k_4} O_2(^3\Sigma) + 2I \tag{4}$$
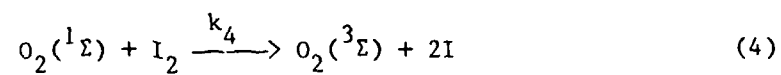
In several recent experiments[9,10] the completeness of that interpretation of I_2 dissociation in the $O_2{}^* - I_2$ system has been questioned; nevertheless, Process (3) is of special importance because the results presented here show it to be one of the critical $O_2(^1\Delta)$ removal processes in the $O_2(^1\Delta) - I$ atom transfer laser.

II. EXPERIMENTAL APPARATUS AND PROCEDURE

A. FLOW SYSTEM

A schematic of the experimental apparatus is shown in Figure 2. The triply concentric reactor consists of a 38.5-mm-i.d. inner Pyrex flow tube surrounded by a jacket for a temperature-controlled recirculating fluid. The outer jacket is then evacuated to prevent frosting under low-temperature operation. A mixture of ethylene glycol and water (50% by volume) was suitable to cover the temperature range -20 to 80°C and is optically transparent in the spectral region of interest (0.6 to 1.4 μm). The flow tube was internally coated with high melting (80°C) halocarbon wax in order to make the surface inert to I atom recombination. Although this procedure does introduce some transmission loss, that loss is not wavelength dependent between 0.6 and 1.4 μm. Differences in coating uniformity caused a correctable variation of less than 5% in the transmission through the 60 cm length of thermostatted flow tube.

Electronically excited oxygen was created by a 2.45-GHz microwave discharge in pure O_2. The $O(^3P)$ atoms produced by the discharge were recombined on a HgO surface[11] formed downstream of the cavity by co-discharging O_2 and Hg vapor prior to an experiment. The absence of NO_2^* emission [$O(^3P)$ + NO impurity] was used to diagnose the removal of $O(^3P)$ from the flow. In a similar system, Derwent and Thrush[6] reported that the $[O(^3P)] < 10^{-6}[O_2]$. As Figure 2 indicates, two Wood's horns were incorporated into the discharge section to suppress scattered light in the main flow tube. An upstream injector for quenching species such as H_2O or NO_2 has been used primarily for studies of the I_2 dissociation mechanism.[10]

The temperature of the gas stream was measured with a moveable thermocouple inserted along the centerline from the downstream end of the flow tube. Under the experimental conditions reported here, the gas temperature agreed with the recirculating bath temperature (±2°C) at positions >8 cm downstream of the radial I_2 injector. All data reported were collected in the constant temperature portion of the flow tube.
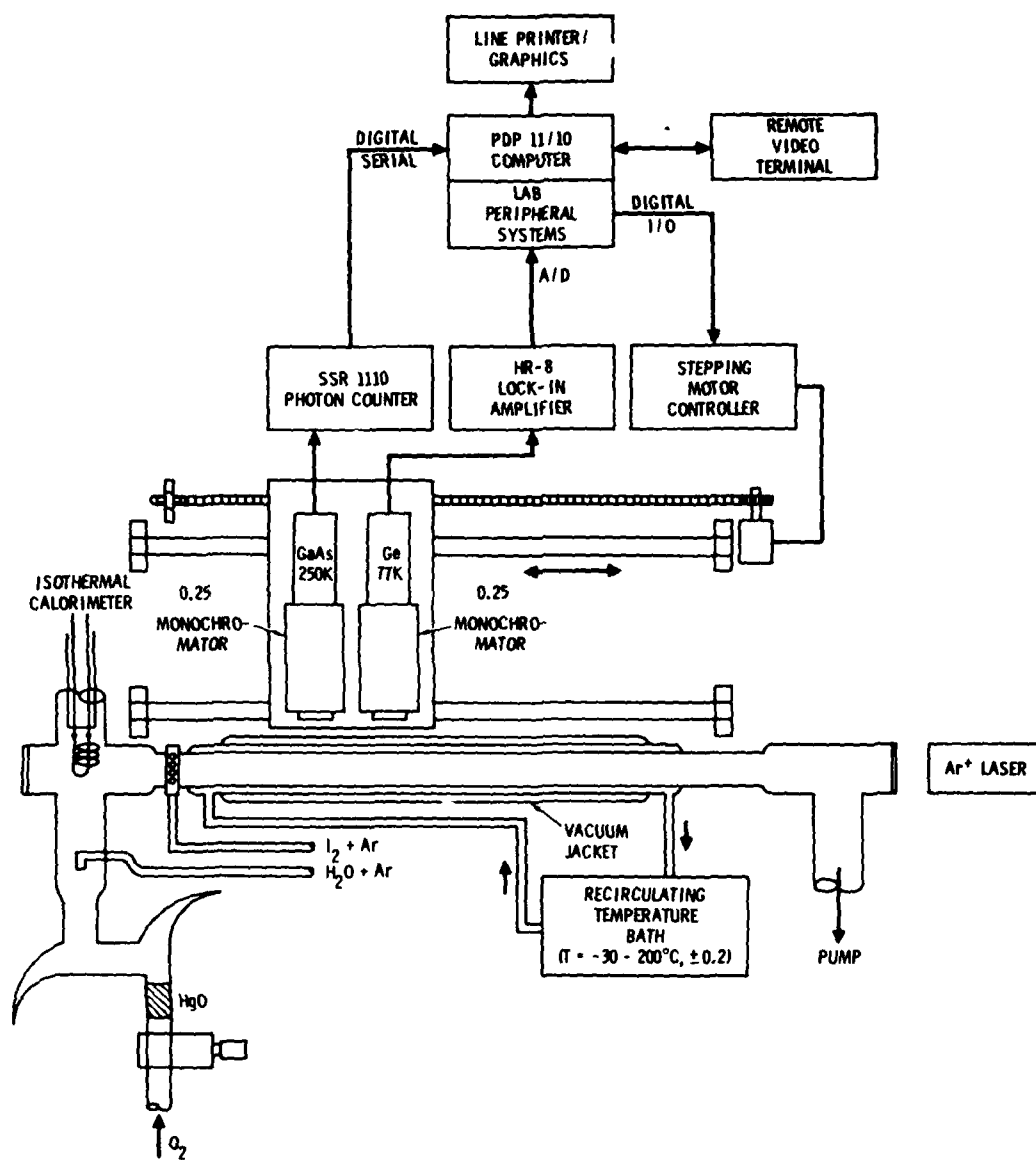
Figure 2. Temperature-Controlled Kinetic Flow-Tube Apparatus

Earlier work in this laboratory[12] on the O_2 - I_2 system established the critical importance of operating under conditions of approximately constant pressure, constant flow velocity, and constant mixing. In order to accomplish the above goals in this study, a stream of Ar was split and separately metered by digital flowmeters (Tylan Corporation) either through a temperature-controlled I_2 saturator or through a bypass line. When these two flows were rejoined at the injector, the total molar flow rate of argon injected was constant, and the mole fraction of I_2 was varied by altering the fraction of argon bypassed around the saturator. Oxygen was metered by a digital flow-meter. The total system pressure was held constant to ±10 mTorr by measuring it with a 0- to 10-Torr capacitance manometer (MKS Tru Torr) with 1-mTorr resolution. The digital flowmeters were calibrated for the specific gas metered and are stated to have a ±2% full-scale accuracy. Although the flow system is not bakable, it was routinely pumped to <5-mTorr pressure with a 15-cfm mechanical pump (Welch 1397), and it exhibited a leak or outgassing rate less than 30 mTorr/hr.

B. MATERIALS

The O_2 (Matheson UHP, 99.99%) and argon (Matheson UHP, 99.9995%) were passed through Linde 5A molecular sieves at 17 psia, primarily to remove impurities from regulators and metal connecting lines. The sieves were out-gassed under vacuum at 200°C before use, and then the sieve traps were cooled to -78°C during experimental measurements. I_2 (ROC/RIC, 99.99%) was sublimed under vacuum onto 3-mm-diameter glass beads. Before each experimental run, the I_2 saturator was extensively purged with high purity argon and then repeatedly pumped down to vacuum.

C. ISOTHERMAL CALORIMETER

The construction, operation, and calibration of the isothermal calorimeter probe has been previously described.[12] The self-balancing Wheatstone bridge circuit reported by Trainor et al.[13] was employed for measuring $O_2(^1\Delta)$. In this method, a nickel wire coil was used to remove a fraction of the excited molecules from the flow. In the absence of excited molecules, an external power supply heats the coil to approximately 150°C. The external power necessary to

15

keep the coil at constant temperature is reduced when $O_2(^1\Delta)$ is deactivated at the coil surface providing 22.7 kcal/mol of energy. The measured power difference is related to the molar flow rate of $O_2(^1\Delta)$ deactivated, since $O(^3P)$ atoms have been removed and $O_2(^1\Sigma)$ is a minority constituent $[<1\%$ of $O_2(^1\Delta)]$. Apparently, Bader and Ogryzlo[11] observed vibrationally excited O_2 on an isothermal probe at short times after the discharge. This $O_2^\dagger$ was removed relative to $O_2(^1\Delta)$ by the addition of H_2O to the flow. By adding approximately 25 mTorr of H_2O to our flow, we have tested for effects traceable to $O_2^\dagger$ or $O_2(^1\Sigma)$ and have found none.

D. SPECTROSCOPY

Two 0.25-m Bausch and Lomb monochromators were mounted on a moveable rail platform driven by a computer-controlled stepping motor (Figure 2). The near-infrared monochromator (1.0-μm blaze grating) was fitted with an intrinsic germanium detector (ADC Model 403 or 403 HS). The radiation from $O_2(^1\Delta)$ at 1.27 μm or I^* at 1.315 μm was chopped at 667 Hz, and the resulting signal from the germanium detector fed to a lock-in amplifier (PAR HR8). When an absolute comparison of the $[I^*]$ to the $[O_2(^1\Delta)]$ was required, the peak heights measured by the low-resolution 0.25-m monochromator were calibrated against peak areas measured by a high-resolution 0.3-m McPherson scanning monochromator fitted with a 1.0-μm blaze grating and utilizing the same detection system. A high-resolution scan is reproduced in Figure 3.

In addition to the optical system just described, a 0.25-m Bausch and Lomb monochromator was used to isolate a number of spectral features within the detection limits of a GaAs photomultiplier (RCA 31034). These features included the $O_2(^1\Delta)$ dimol peaks at 6340 and 7030 Å, the $O_2(^1\Sigma)$ emission at 7619 Å, and the $I_2(B \rightarrow X)$ emission that peaks roughly at 5800 Å. These signals were amplified and discriminated (SSR 1120) and then accumulated in a photon counter (SSR 1110). In a pure O_2 system, the $O_2(^1\Sigma)$ peak at 7619 Å is so intense that it must be attenuated by a neutral density filter to avoid scattered light problems in the monochromator and saturation in the pulse amplifier.

The system densities were placed on an absolute basis using the following procedure. The dimol emission signal at 6340 Å and the $O_2(^1\Delta)$ fundamental
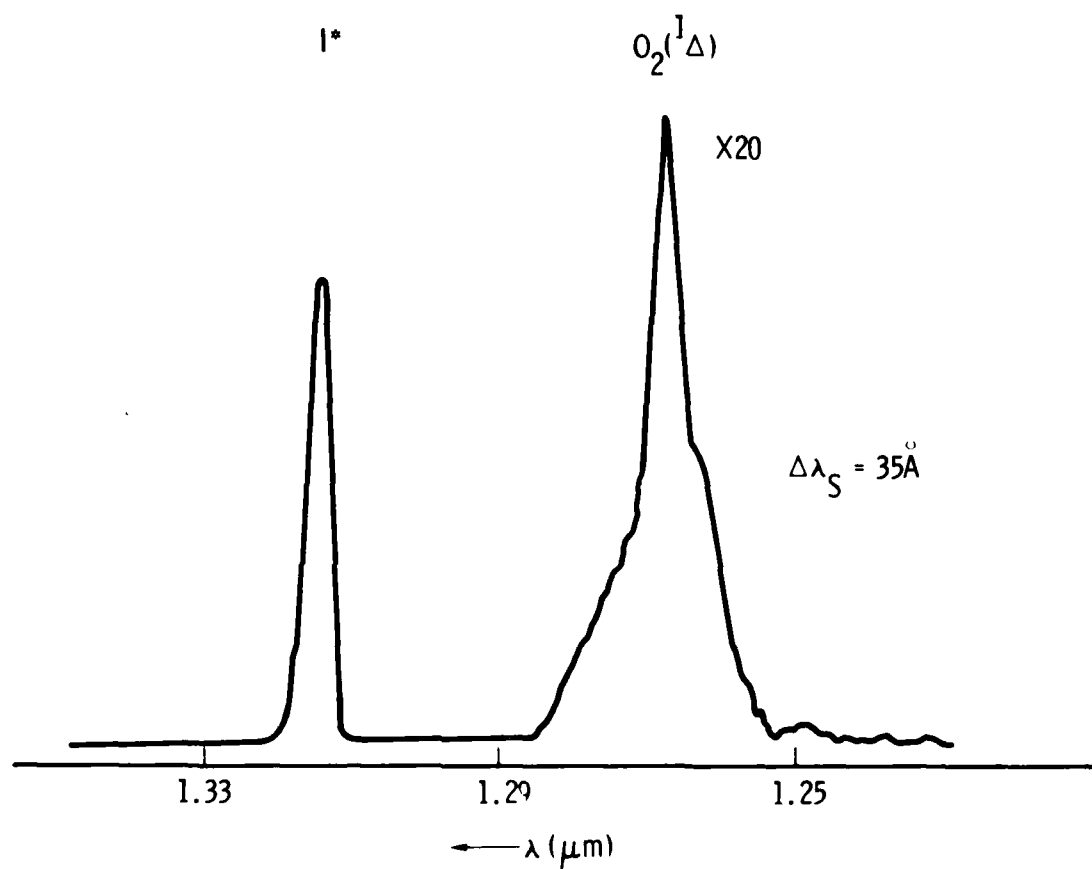
Figure 3. Medium Resolution Spectral Scan of $O_2(^1\Delta \rightarrow {}^3\Sigma)$ and $I(^2P_{1/2} \rightarrow {}^2P_{3/2})$ Transitions

emission were directly calibrated against the isothermal calorimeter. Derwent and Thrush[6] used a nearly identical method to determine the dimol emission rate, k_R

$$O_2(^1\Delta) + O_2(^1\Delta) \xrightarrow{\ k_R\ } O_2(^3\Sigma) + O_2(^3\Sigma) + h\nu \qquad \lambda = 6340 \text{ Å} \qquad (5)$$
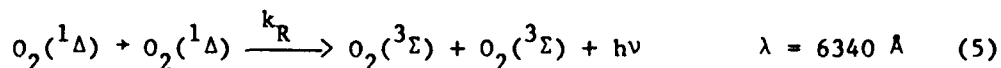
and we employed this value to estimate an absolute $[O_2(^1\Sigma)]$:

$$[O_2(^1\Sigma)] = T_1 \frac{k_R}{A_{7619}} \frac{I_{7619}}{I_{6340}} [O_2(^1\Delta)]^2 \qquad (6)$$

The term T_1 is an optical throughput or detectivity correction between these wavelengths measured with a blackbody source, and A_{7619} is the $O_2(^1\Sigma)$ Einstein coefficient (0.077 s^{-1}).[14]

Because of strong pumping from $O_2(^1\Delta)$ [Process (1)], I^* is rather homogeneously distributed throughout the flow tube. Its concentration can be absolutely evaluated by comparing the relative intensities at 1.315 μm (I^*) and 1.27 μm $[O_2(^1\Delta)]$,

$$[I^*] = T_2 \frac{A_{1.27}}{A_{1.315}} \frac{I_{1.315}}{I_{1.27}} [O_2(^1\Delta)] \qquad (7)$$

where T_2 is the throughput or detectivity correction, and $A_{1.27}$ and $A_{1.315}$ are the Einstein coefficients for $O_2(^1\Delta)$ ($2.7 \times 10^{-4} \text{ s}^{-1}$)[15] and I^* (7.8 s^{-1}),[16] respectively. An independent method for calculating the $[I^*]$ has also been used. If one assumes or demonstrates complete I_2 dissociation, $[I^*] + [I] = 2[I_2]_0$. The equilibrium ratio $[I^*]/[I]$ can be determined from Process (1) ($K_{EQ} = k_1/k_{-1}$) by statistical mechanics for a measured ratio of $O_2(^1\Delta)/O_2(^3\Sigma)$ if certain kinetic constraints are obeyed.[8] Thus,

18

$$[I^*] = 2[I_2]_0\left(\frac{x}{1 + x}\right) \tag{8}$$

where $x = K_{EQ}[{}^1\Delta]/[{}^3\Sigma]$. The agreement between these two determinations of $[I^*]$ will be discussed later.

E. ON-LINE COMPUTER SYSTEM

By means of a stepping motor and chain drive mechanism, a PDP 11/10 minicomputer directs the movement of the spectroscopy table to preset positions along the flow tube. For the data reported for k_2, 50 positions are sampled at intervals of approximately 1 cm. Each stepping motor pulse advances the platform 0.02 cm. In addition, the computer acquires digital output data from the photon counter and performs an analog-to-digital (A/D) conversion on the analog output of the lock-in amplifier. All physical parameters necessary for the data analysis (e.g., pressures, temperatures, and molar flow rates) are entered by means of a remote video terminal. An interactive data acquisition program maintains the system calibration programs and archives the output data files onto hard disk and cassette tape. These data files are analyzed by various curve-fitting routines that are discussed in Section III. Hardcopy plots are obtained on a line printer (Printronix 300) using commercial graphics software (Cerritos Corporation).

III. DATA ANALYSIS AND EXPERIMENTAL RESULTS

A. $O_2(^1\Delta) + O_2(^1\Delta)$ POOLING

The procedure used for measuring the relative pooling rate coefficient k_2 as a function of temperature is a modification of that used by O'Brien and Myers[17] to measure $O_2(^1\Sigma)$ quenching. The same mathematical analysis was used by Borrell et al.[18,19] for high-temperature $k_2(T)$ measurements by a discharge flow/shock tube technique. In addition to k_2, the following processes must be considered:

$$O_2(^1\Sigma) + \text{wall} \xrightarrow{k_9} O_2(^1\Delta) + \text{wall} \tag{9}$$

$$O_2(^1\Sigma) + M \xrightarrow{k_{10}^M} O_2(^1\Delta) + M \tag{10}$$

$$O_2(^1\Delta) + \text{wall} \xrightarrow{k_{11}} O_2(^3\Sigma) + \text{wall} \tag{11}$$

$$O_2(^1\Delta) + M \xrightarrow{k_{12}^M} O_2(^3\Sigma) + M \tag{12}$$
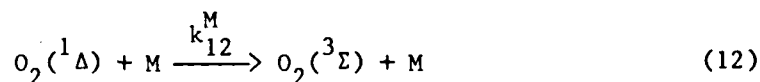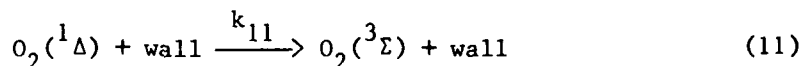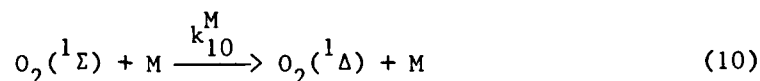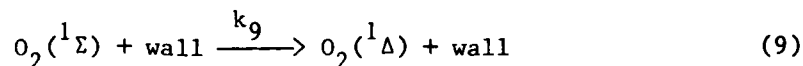
If the time-dependent $[O_2(^1\Sigma)]$ is determined from Eqs. (2) and (9) through (12), one obtains

$$[^1\Sigma] = \frac{k_2[^1\Delta_0]^2}{k_\Sigma - 2k_\Delta} \exp(-2k_\Delta t) - \left\{ \frac{k_2[^1\Delta_0]^2}{(k_\Sigma - 2k_\Delta)} - [^1\Sigma_0] \right\} \exp(-k_\Sigma t) \tag{13}$$

where $k_\Sigma = k_9 + \sum k_{10}^M [M]$ and $k_\Delta = k_{11} + \sum k_{12}^M [M]$. In addition, the expression $[^1\Delta] = [^1\Delta_0^M] \exp(-k_\Delta t)$ has been used. In previous work,[17] the approximation $k_\Sigma \gg 2k_\Delta$ was made, which is equivalent to assuming that $O_2(^1\Sigma)$ is in steady state. The exact expression will be retained here, although in the present apparatus, $k_\Sigma \geq 25\, k_\Delta$. Examination of Eq. (13) shows that the second pre-exponential term is zero if the $O_2(^1\Sigma)$ is nearly in steady state. In that event, $O_2(^1\Sigma)$ decays with twice the rate coefficient of $O_2(^1\Delta)$. If that condition is perturbed, the $O_2(^1\Sigma)$ recovers with a time constant $\tau = k_\Sigma^{-1}$.

Using the technique developed by O'Brien and Myers,[17] the flow was modified by inserting a flat aluminum wire spiral (~50% coverage). The coil deactivates 20 to 50% of the $O_2(^1\Sigma)$ (depending upon flow velocity) without affecting $O_2(^1\Delta)$. An example of the resulting kinetic curve is shown in Figure 4. Nonlinear fits to these curves were made using the functional form

$$I(t) = A \exp(-Bt) + C \exp(-Dt) \tag{14}$$

where $I(t)$ is the time-dependent $O_2(^1\Sigma)$ emission at 7619 Å, $A \equiv [k_2(^1\Delta_0)^2/(k_\Sigma - 2k_\Delta)]$, $C \equiv A - [^1\Sigma_0]$, $B \equiv 2k_\Delta$, and $D \equiv k_\Sigma$. By rearranging these definitions, we obtain

$$k_2 = \frac{\alpha A(D - B)}{[^1\Delta_0]^2} \tag{15}$$

where α is a constant that can be approximated from Eq. (6) or determined from some other absolute calibration for $O_2(^1\Sigma)$ if absolute values of k_2 are desired. In Table I, the values of $k_2(T)$ are reported relative to $k_2(295)$ values determined in this study. Derwent and Thrush[6] had previously determined the absolute value $k_2(295) = (2.0 \pm 0.5) \times 10^{-17}$ cm^3/molecule-sec. Because relative values of $k_2(T)/k_2(295)$ are reported in Table I, the term α in Eq. (15) need not be determined. In addition, one can measure the relative $O_2(^1\Delta)$ fundamental emission intensity at the two temperatures instead of determining the $[^1\Delta_0]$ absolutely. Thus, the estimated error of ±25% quoted in Table I reflects the fitting error of the parameters A, B, and D from Eq. (14) at the two temperatures (T and 295 K). The parameter D is by far the major source of error.

The rate coefficient determined at T = 295 K has been normalized to unity at each of the four pressures studied. Subsequent to that procedure, Table I does indicate some variation of k_2 with pressure at temperatures other than 295 K; however, this variation is probably not significant. The average of the $k_2(T)/k_2(295)$ values at the four pressures studied is reported in Table I and plotted in Figure 5. By definition, the present value of $k_2(295)$ is normalized to that reported in Ref. 6 and plotted in Figure 5.

22
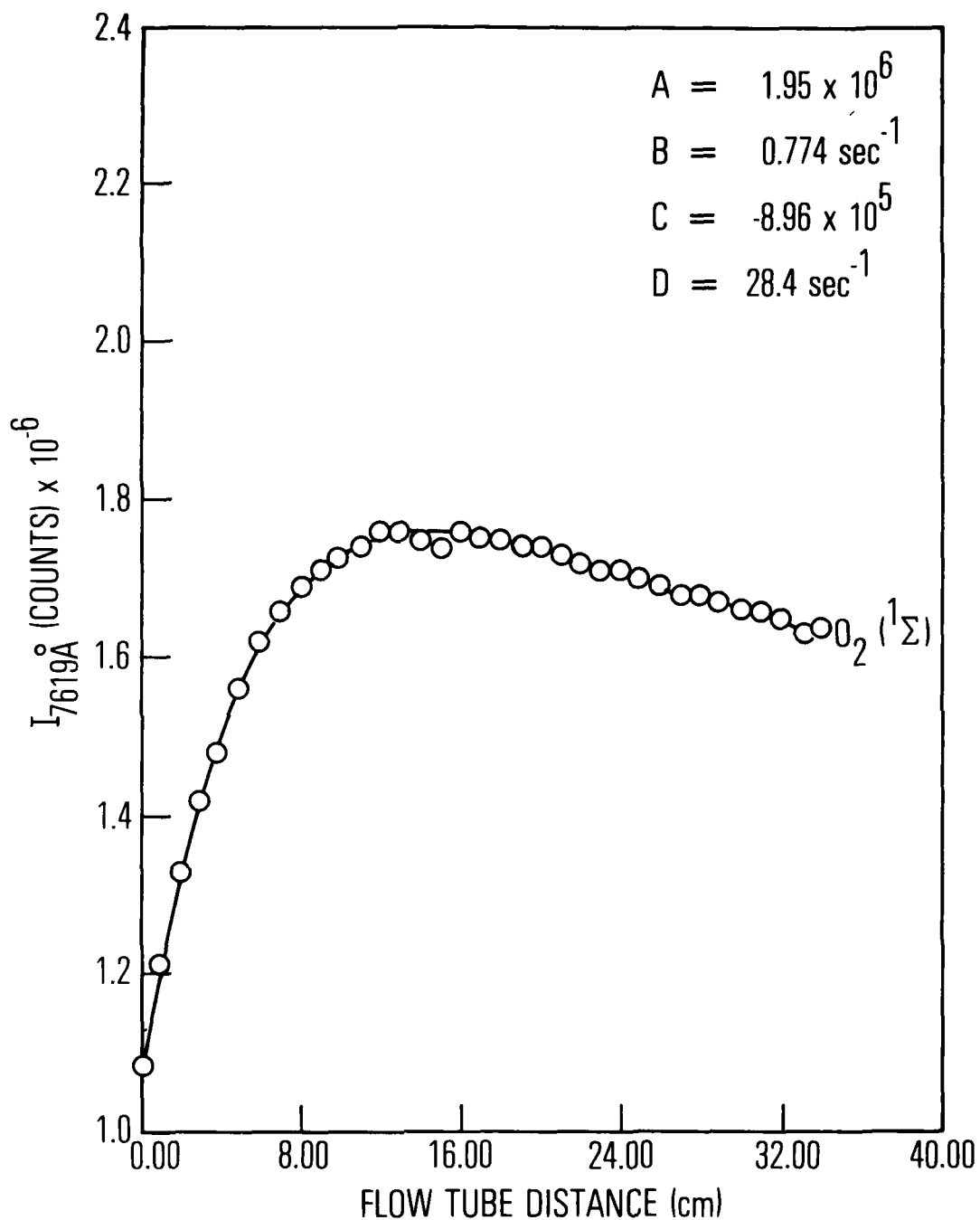
Figure 4. Recovery of $O_2(^1\Sigma)$ to Steady State Following
Selective Deactivation of O_2^* on Aluminum-Wire
Coil. P = 4.00 Torr, T = 295 K, flow velocity =
145 cm/sec. Experimental data (O); computer fit
to Eq. (14) (———).
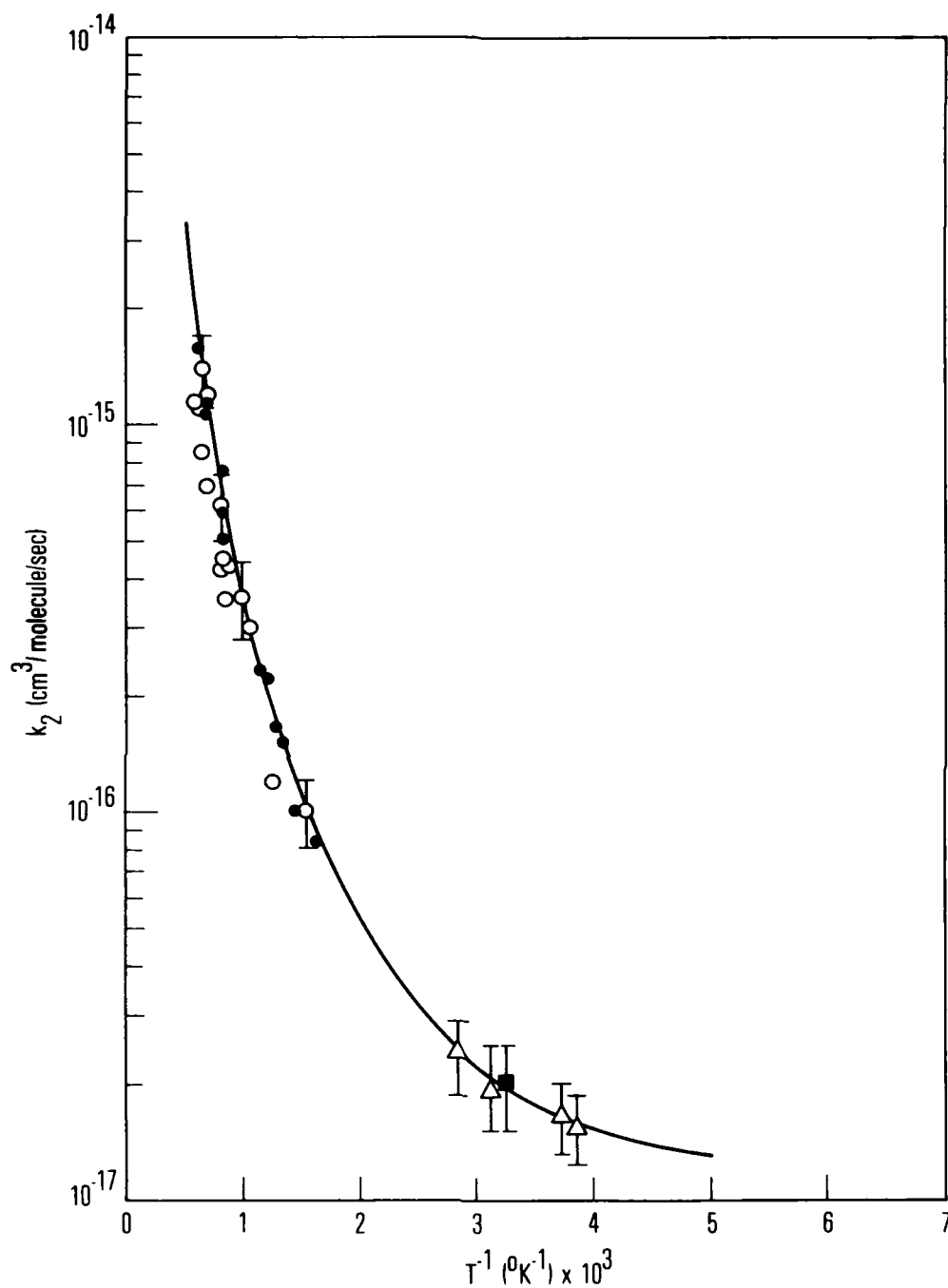
Figure 5. Arrhenius Plot of ln k_2 Versus T^{-1}. Ref. 6 (■); Ref. 19 (●O_2/N_2 mixtures, pure O_2); this work (△). The fitted curve (———) is k_2 (T) = $7.0 \times 10^{-28} T^{3.8}$ exp (700/T). Ref. 19 points (◯) are not included in the fit.

24

Table I. Experimental Values for $k_2(T)/k_2(295)$[a]
as a Function of Total System Pressure

P (Torr)	259	268	T (K) 295	320	352
1.0		0.75[b]	0.87	1.0	0.98	1.2
2.0		0.67	0.72	1.0	0.98	1.2
3.0		0.78	0.86	1.0	0.91	1.2
4.0		0.86	0.88	1.0	0.92	1.2
Avg	0.77	0.83	1.0	0.95	1.2

[a]$k_2(295) = (2.0 \pm 0.5) \times 10^{-17}$ cm^3/molecule-sec (Ref. 6).
[b]Total error (random and systematic) estimated to be $\pm 25\%$ for all tabulated values.

These data are compared with the limited temperature-dependent information available for k_2 in Table II and then plotted on an Arrhenius scale in Figure 5. The nature of the quenching of $O_2(^1\Sigma)$, k_Σ, is shown in Figure 6. Unlike previous flow-tube studies[6] where the walls were the dominant quencher of $O_2(^1\Sigma)$, the wall removal rate in the present study appears to be independent of pressure rather than diffusion controlled, i.e., $k_9 = \bar{c}\gamma/2R \approx 6$ sec^{-1}, where R is the flow-tube radius, $\bar{c}$ is the molecular velocity, and γ is the wall-deactivation coefficient. Ignoring the slight variation of $\bar{c}$ with temperature, the data support $\gamma \approx 1.1 \times 10^{-3}$ instead of the typical[6] $\gamma \approx 1 \times 10^{-2}$. This must be a property of the halocarbon wax coating since previous measurements used bare or acid-washed Pyrex and quartz.

The slope of the linear fit in Figure 6 gives $k_{10}^{O_2} = 1.4 \times 10^{-16}$ cm^3/molecule-sec, whereas the accepted result from laser-induced fluorescence[20,21] is 4×10^{-17} cm^3/molecule-sec. The present result is typical of discharge-flow-system results, where it is generally presumed that H_2O impurity causes the higher result. In addition, the $[O_2(^1\Delta)]$ (approximately 5×10^{15}/cm^3) is sufficiently high that it may be a significant quencher of $O_2(^1\Sigma)$. Although the experiment is poorly posed to measure $O_2(^1\Delta)$ removal rates accurately, the
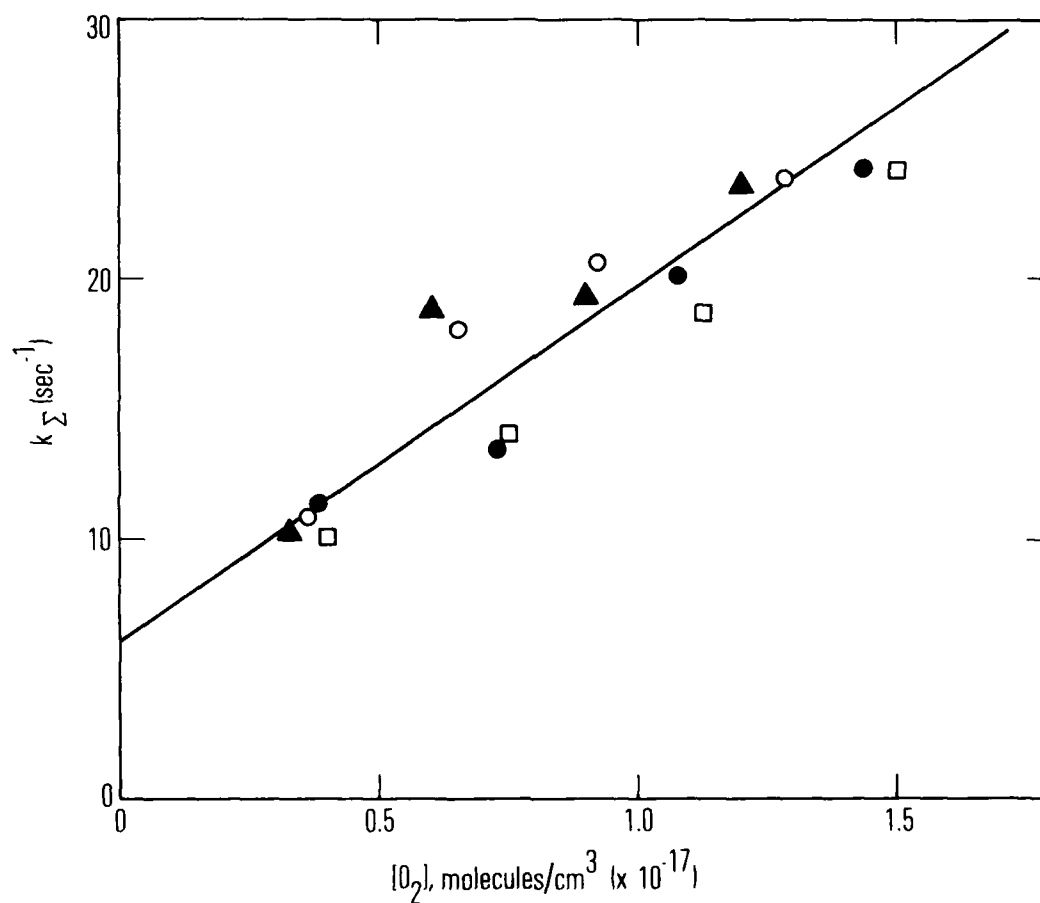
Figure 6. Variation of Total $O_2(^1\Sigma)$ Removal Rate (k_Σ) with O_2 Density: $T = 259$ K (●); $T = 295$ K (○); $T = 320$ K (□); $T = 268$ K(Δ).

Table II. Rate Coefficients for $O_2(^1\Delta)$ Energy Pooling

T (K)	$k_2(T)^a$ $(cm^3/molecule\text{-}sec)$	$k_2(T)/k_2(295)$	Reference
295	$(2.0 \pm 0.5) \times 10^{-17}$	1.0	6
259	$(1.5 \pm 0.4) \times 10^{-17}$	0.77	This work
268	$(1.7 \pm 0.4) \times 10^{-17}$	0.83	This work
320	$(1.9 \pm 0.5) \times 10^{-17}$	0.95	This work
353	$(2.4 \pm 0.6) \times 10^{-17}$	1.2	This work
650	$(1.0 \pm 0.2) \times 10^{-16}$	5.0	19[b]
1000	$(3.6 \pm 0.8) \times 10^{-16}$	18	19
1200	$(6.2 \pm 1.2) \times 10^{-16}$	31	19
1500	$(1.4 \pm 0.3) \times 10^{-15}$	70	19

[a] All values in this column calculated relative to the first entry (Ref. 6). The error quoted for $k_2(295)$ is not reflected in the absolute $k_2(T)$ values quoted.

[b] Additional measurements from Ref. 19 are plotted in Figure 5.

fitting parameter $B \equiv 2 k_\Delta$ in Eq. (14) gives $^1\Delta$ decays [i.e., $k_\Delta \approx (0.4 \pm 0.2)sec^{-1}$] that are in good agreement with the recent study by Borrell et al.[22] and with $O_2(^1\Delta)$ fundamental emission decays in the present system measured at low plug flow velocities (<40 cm/sec). Thus, we have confidence in the method despite the very small T-dependence measured for k_2.

B. $\underline{O_2(^1\Delta) + I^* \text{ POOLING}}$

When I_2 is injected into a flow of $O_2(^1\Delta)$ and $O_2(^1\Sigma)$, it is rapidly dissociated into atoms.[1,5,7] This process is apparently more complex than previously reported,[7] and details of recent work performed in this laboratory will be published elsewhere.[10] Regardless, the behavior of $O_2(^1\Sigma)$ is strongly modified by the presence of free iodine atoms that are pumped to I^* by Process (1). As the data presented here show, k_3 is much larger than k_2, resulting in an increase in the steady state $[O_2(^1\Sigma)]$ even for small ratios of $[I^*]/[^1\Delta]$.

This phenomenon was extensively reported in earlier studies.[1,8] The time-dependent behavior of $O_2(^1\Sigma)$ following I_2 injection (Figure 7) clearly resembles the aluminum-wire perturbation curve (Figure 4) in the pure O_2 system. If I_2 mixing and dissociation were instantaneous on the time scale of the rise to a new steady state $[O_2(^1\Sigma)]$, an analog of Eq. (13) could be used to analyze the data. Although that method has been attempted, we have primarily relied on an extension of the steady-state method used by Derwent and Thrush[8] to measure the ratio k_3/k_2. In the absence of I_2, the steady-state density of $O_2(^1\Sigma)$ is given by

$$[^1\Sigma_0]_{ss} = \frac{k_2[^1\Delta_0]^2}{k_\Sigma} \tag{16}$$

where $k_\Sigma = k_9 + \sum_M k_{10}^M[M]$. In the presence of I_2

$$[^1\Sigma]_{ss} = \frac{(k_2 + k_3[I^*]/[^1\Delta])[^1\Delta]^2}{k_\Sigma'} \tag{17}$$

where $k_\Sigma' = k_\Sigma + \sum_M k_{10}^M[M']$ ($M' = I_2$, I, and I^*). We can write the following extension of the Derwent and Thrush[8] analysis by ratioing Eqs. (17) and (16):

$$\frac{[^1\Sigma]_{ss}}{[^1\Sigma_0]_{ss}} \cdot A \cdot B = \left(1 + \frac{k_3}{k_2}\frac{[I^*]}{[^1\Delta]}\right) \tag{18}$$

where $A \equiv ([^1\Delta_0]/[^1\Delta])^2$ and $B \equiv k_\Sigma'/k_\Sigma$.

The term $A \neq 1$ allows for $O_2(^1\Delta)$ deactivation by iodine-containing species between the mixing point and the fixed detection point after steady state is established. The term $B \neq 1$ allows for additional $O_2(^1\Sigma)$ quenching by the iodine-containing species. This additional quenching would be manifested in plots such as Figure 7 or by nonlinearity in plots of $([^1\Sigma]_{ss}/$
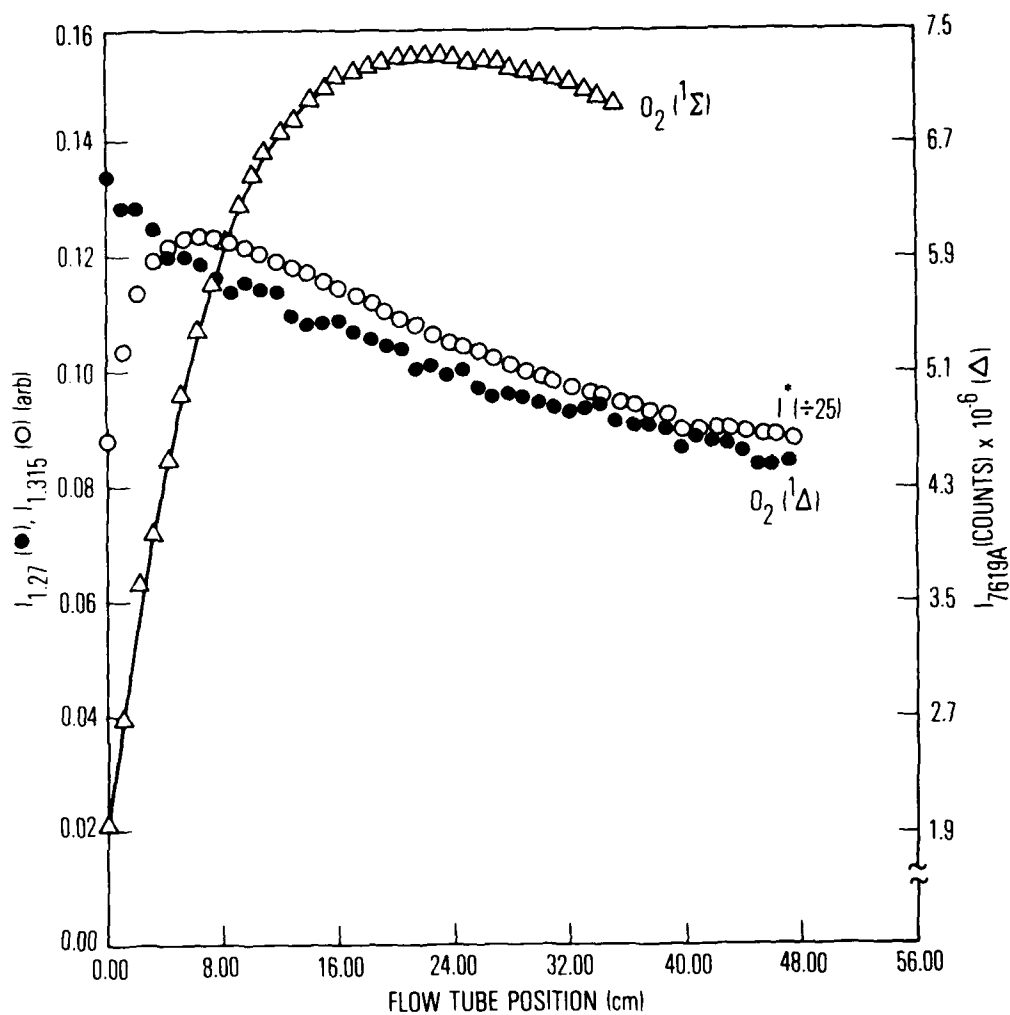
28

Figure 7. Time Dependence of I^*, $^1\Delta$, and $O_2(^1\Sigma)$ Following I_2 Injection into O_2: P = 3.45 Torr, T = 354 K, Flow Velocity = 279 cm/sec. $O_2(^1\Sigma)$ data fitted by Eq. (14) (A = 8.89×10^6; B = 1.76 sec^{-1}; C = -6.93×10^6; D = 34.1 sec^{-1}).

29

$[^1\Sigma_0]_{ss}$) A − 1 versus $[I^*]/[^1\Delta]$. We chose to plot $[I^*]/[^1\Delta]$ ratios that are determined by Eq. (7) (spectroscopic based on Einstein coefficients) rather than by Eq. (8) (I^* is determined by flow rate analysis and the equilibrium constant $K_{EQ} = k_1/k_{-1}$). The former method provides $[I^*]/[^1\Delta]$ values 30% smaller than the latter method in our present system. Systematic errors in both methods prevent an unambiguous choice.

The experimental data for determining k_3/k_2 by Eq. (18) are presented in Figures 8 and 9. These data represent runs at different I_2 saturator temperatures and, thus, translate into different ranges of the addition of I_2 to the O_2^* flow. We obtained data at much larger [I] and $[I^*]$ than did Derwent and Thrush.[8] Figure 7 shows that for large $[I^*]$, approaching the levels pertinent to the $O_2(^1\Delta)$ − I atom transfer laser, $[O_2(^1\Delta)]$ decays substantially prior to $O_2(^1\Sigma)$ reaching steady state, yet the plots in Figures 8 and 9 remain linear after the correction for A > 1 is applied. The exception are the data at T = 268 K, where we believe that B > 1 at high ratios of $[I^*]/[^1\Delta]$. Using the recent laser-induced fluorescence measurement[9] for $O_2(^1\Sigma)$ removal by I_2 of 2.0 × 10^{-11} cm^3/molecule-sec, we estimate that the data in Figure 8 at T = 268 K can be explained by <1% undissociated I_2.

Further work at low temperatures and large $[I^*]$ would be interesting if iodine species do not condense either in the gas phase or at the walls. The results for k_3/k_2 are summarized in Table III. The statistical error for k_3/k_2 cited in Table III is quite small in most cases. The systematic error inherent in making the relatively large correction for the term A in Eq. (18) is quite significant. Although systematic errors traceable to the term B in Eq. (18) should result in smaller k_3/k_2 values at the higher $[I_2]$ addition range, an opposite trend of ~10% is observed (Table III). Given the assumptions regarding steady state and the accuracy with which the I^* and $^1\Delta$ intensities could be measured, the relative k_3/k_2 values versus temperature are estimated to have a total uncertainty (random and systematic) of ±20%. In addition, the absolute values of k_3/k_2 are subject to the uncertainty discussed above and in Footnote (a) of Table III. An estimate of $k_3(T)$ is made using the values of $k_2(T)/k_2(295)$ in Table IV. Clearly, k_3/k_2 is not temperature-dependent in the range T = 268 to 353 K.

40

353 K

320 K

30

298 K

$(|^1\Sigma|/|^1\Sigma_0|) \cdot A - 1$

268 K

20

10

0

0   10   20   30   40

$|I^*|/|^1\Delta| \times 10^4$

Figure 8. Analysis of $O_2(^1\Sigma)$ Enhancement by Process (3).
Data plotted according to Eq. (17) with
B = 1. $[I_2]_0 = 0 - 5.8 \times 10^{13}$ molecules/cm^3.
Solid points: 2.0 Torr; Open points:
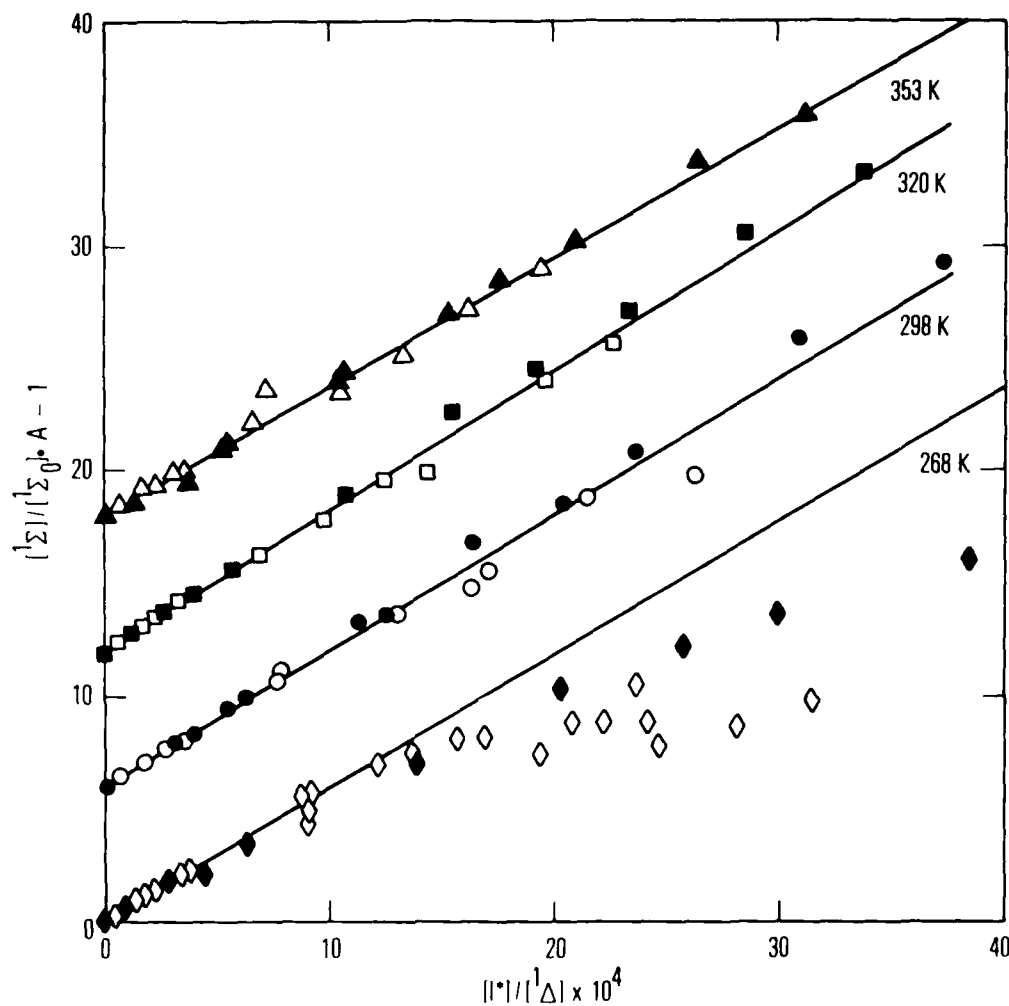3.6 Torr. Nonzero intercepts are artificial
for clear display.

31
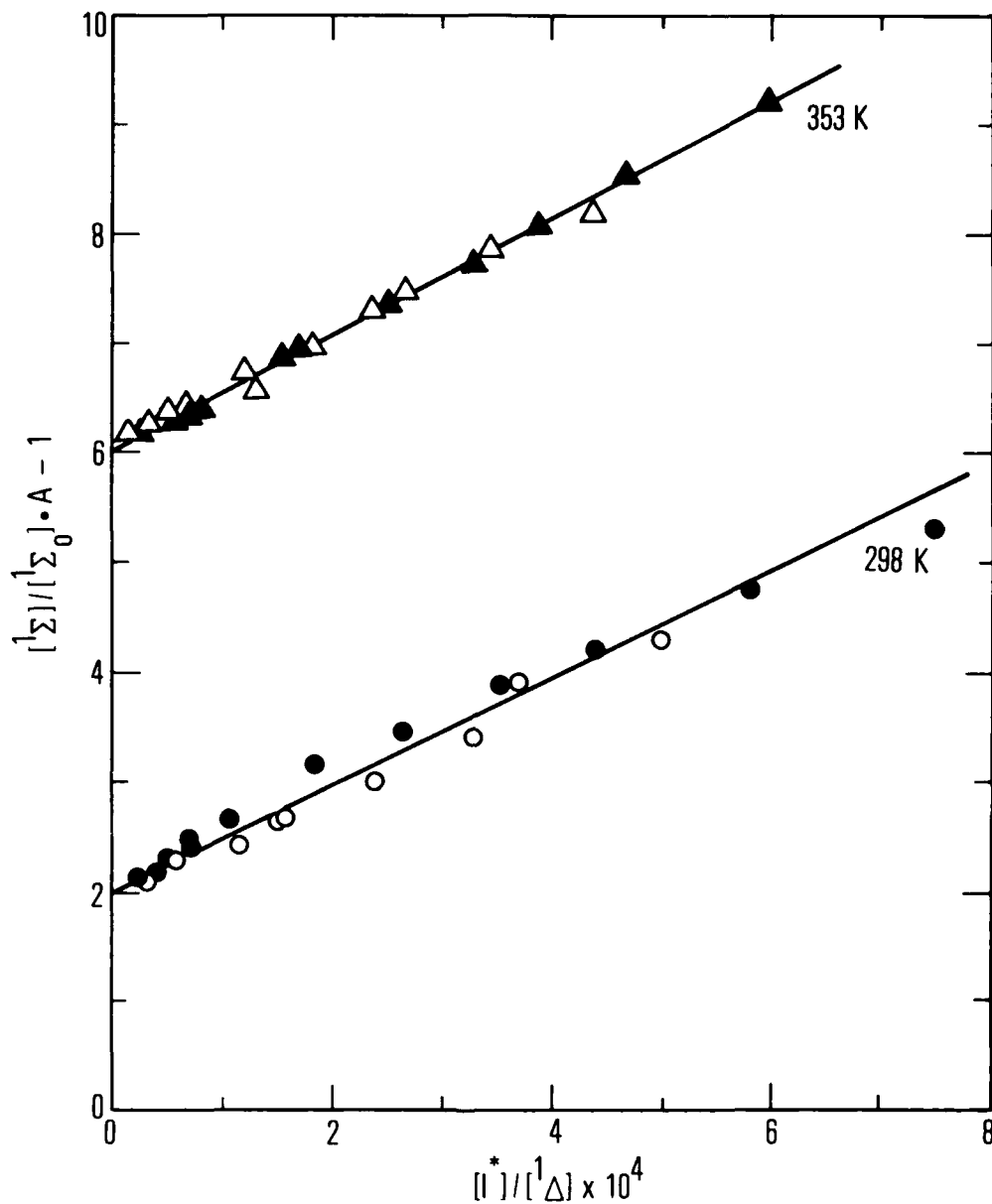
Figure 9. Analysis of $O_2(^1\Sigma)$ Enhancement by Process (3). Data plotted according to Eq. (17) with B = 1. $[I_2]_0 = 0 - 1.2 \times 10^{13}$ molecules/cm^3. Solid points: 2.0 Torr; Open points: 3.6 Torr. Nonzero intercepts are artificial for clear display.

Table III. Experimental Values for $k_3(T)/k_2(T)$[a,b] as a Function of Total Pressure and $[I_2]$

P (Torr)	T (K)			
	268	298	320	353
2.0[c]	$(5.8 \pm 0.5) \times 10^3$	$(6.3 \pm 0.1) \times 10^3$	$(6.4 \pm 0.1) \times 10^3$	$(5.9 \pm 0.1) \times 10^3$
2.0[d]		$(5.0 \pm 0.4) \times 10^3$		$(5.4 \pm 0.1) \times 10^3$
3.6[c]	$(5.0 \pm 0.5) \times 10^3$	$(5.4 \pm 0.1) \times 10^3$	$(6.0 \pm 0.1) \times 10^3$	$(5.5 \pm 0.1) \times 10^3$
3.6[d]		$(4.7 \pm 0.2) \times 10^3$		$(4.9 \pm 0.2) \times 10^3$

[a]The term $[I^*]/[^1\Delta]$ required for the plots in Figures 8 and 9 is calculated from spectroscopic data [Eq. (7)]. If this term had been calculated using mass balance [Eq. (8)], all entries would be ~30% lower (~4 × 10³).
[b]Errors quoted represent 1 σ for the plots in Figs. 8 and 9.
[c]I_2 addition range: 0 – 5.8 × 10¹³ molecules/cm³.
[d]I_2 addition range: 0 – 1.2 × 10¹³ molecules/cm³.

33

Table IV. Rate Coefficients for $O_2(^1\Delta) + I^*$ Energy Pooling

T (K)	$k_3(T)^a$ (cm^3/molecule-sec)	$\dfrac{k_3(T)}{k_2(T)}$	Reference
295	$(2.7 \pm 0.3) \times 10^{-14b}$	1.3×10^{3b}	8
298	$(8.3 \pm 1.7) \times 10^{-14}$	4.2×10^3	12
298	$<2.2 \times 10^{-13}$	–	12
268	$(0.9 \pm 0.3) \times 10^{-13}$	$(5.4 \pm 1) \times 10^{3c}$	This work
298	$(1.1 \pm 0.3) \times 10^{-13}$	$(5.4 \pm 1) \times 10^{3c}$	This work
320	$(1.2 \pm 0.4) \times 10^{-13}$	$(6.2 \pm 1) \times 10^{3c}$	This work
353	$(1.3 \pm 0.4) \times 10^{-13}$	$(5.4 \pm 1) \times 10^{3c}$	This work

[a]$k_2(295) = (2.0 \pm 0.5) \times 10^{-17}$ cm^3/molecule-sec (Ref. 6) is assumed in order to calculate $k_3(T)$.

[b]Although the abscissa of Figure 3 of Ref. 8 is mislabeled, the authors have confirmed their reported value for k_3.

[c]See Footnote (a) in Table III for discussion of a possible 30% systematic error.

IV. DISCUSSION

The present study, an earlier more qualitative study in this laboratory,[12] and a recent determination[23] by an independent technique have all provided a relative rate coefficient ratio of $k_3/k_2 = (5.0 \pm 1.0) \times 10^3$ at T = 295 K. This result is in rather poor agreement with the widely accepted determination by Derwent and Thrush.[8] That value was quoted as 1.3×10^3 (see Footnote (b) of Table IV). When this result is combined with the measurement[6] $k_2 = (2.0 \pm 0.5) \times 10^{-17}$ cm^3/molecule-sec (T = 295 K) by the same authors, the resulting value of k_3 is $(2.7 \pm 0.3) \times 10^{-14}$ cm^3/molecule-sec. The present data support a room-temperature value of $k_3 = (1.1 \pm 0.3) \times 10^{-13}$ cm^3/molecule-sec when combined with the same k_2 value. Most of the assumptions (A = 1, B = 1) made by Derwent and Thrush[8] would result in their obtaining too large a value for k_3. We previously reported[12] a semiquantitative upper bound for k_3 based on separating the first- and second-order components of $O_2(^1\Delta)$ removal in the presence of large I* densities (Table IV). That measurement was $k_3 < 2 \times 10^{-13}$ cm^3/molecule-sec, with $O_2(^1\Sigma)$ assumed to be predominantly quenched to $O_2(^1\Delta)$ and not to $O_2(^3\Sigma)$.

The discharge flow/shock tube experiment of Borrell et al.[18,19] has provided an impressive amount of temperature-dependent data for Process (2) between 650 and 1650 K. The most remarkable feature of these data is that the energy-pooling process, k_2, and the gas-phase quenching of $O_2(^1\Sigma)$, k_{10}^M, by O_2 and N_2 have large and virtually identical dependencies on temperature. The data for k_2 are plotted in Figure 5 along with the results of the present study. The highly non-Arrhenius nature of these data can be described by an equation of the form $k(T) = AT^n \exp(E/T)$, in particular, $k_2(T) = 7.0 \times 10^{-28}T^{3.8} \exp(700/T)$. The data from the present study can be adequately described by $k_2(T) = (7 \pm 3) \times 10^{-17} \exp(-780/RT)$.

For the pooling Process (2), Schurath[24] has clearly shown a resonant enhancement for producing $O_2(^1\Sigma)$ (v = 2) + $O_2(^3\Sigma)$ (v = 0) at T = 295 K. Steinfeld and Sutton[25] found a very weak temperature dependence for near resonant electronic energy transfer with the use of an approximate surface-

hopping model. It is tempting to argue that these processes dominate the low-temperature data presented here for k_2, whereas collisions on the repulsive part of the interaction potential are responsible for the data presented by Borrell et al.[18,19] Additional data between 350 to 650 K and below 260 K would be useful in testing theoretical models for this highly interesting pooling process. We are also interested in determining whether k_3/k_2 remains temperature independent at high temperatures.

Processes (2) and (3) played a central role in early $O_2(^1\Delta)$ - I atom laser modeling. Because Process (4) was believed to be the sole mechanism for I_2 dissociation, the requisite $[O_2(^1\Sigma)]$ was produced initially by Process (2) and then strongly supplemented by Process (3) as I^* appeared in the system. As stated in the Introduction, new evidence[9,10] points to additional mechanisms that dominate I_2 dissociation in the transfer laser system. Nevertheless, both energy-pooling processes discussed represent second-order kinetic loss terms for $O_2(^1\Delta)$. In particular, $k_3(T)$ provides a serious constraint for scaling the $[I^*]$ without producing an unacceptably large rate for $O_2(^1\Delta)$ decay. Because threshold for the continuous-wave $O_2(^1\Delta)$ - I atom transfer laser occurs for $O_2(^1\Delta)/O_2(^3\Sigma) = 0.17$ at T = 295 K, modest deactivation of $O_2(^1\Delta)$ can represent a substantial loss of laser efficiency.

V. CONCLUSIONS

The temperature-dependent rate coefficients, k_2 and k_3, for electronic-energy pooling have been measured between 259 and 353 K. A comparison to previous results, particularly the works of Derwent and Thrush[6,8] and Borrell et al.,[18,19] was made. Both k_2 and k_3 have weak temperature dependencies (less than 1 kcal/mol) in this temperature range, although there is good evidence for extreme non-Arrhenius behavior for k_2 at elevated temperatures.[18,19] The absolute magnitude of $k_3 [\sim 1 \times 10^{-13}$ $cm^3/molecule\text{-}sec]$ makes it very important for accurately modeling the $O_2(^1\Delta)$-I atom transfer laser.

REFERENCES

1. S. J. Arnold, N. Finlayson, and E. A. Ogryzlo, J. Chem. Phys. 44, 2529 (1966).

2. R. G. Derwent and B. A. Thrush, Chem. Phys. Lett. 9, 591 (1971).

3. W. E. McDermott, N. R. Pchelkin, D. J. Benard, and R. R. Bousek, Appl. Phys. Lett. 32, 469 (1978).

4. A. T. Pritt, Jr., R. D. Coombe, D. Pilipovich, R. I. Wagner, D. Benard, and C. Dymek, Appl. Phys. Lett. 31, 745 (1977).

5. R. G. Derwent, D. R. Kearns, and B. A. Thrush, Chem. Phys. Lett. 6, 115 (1970).

6. R. G. Derwent and B. A. Thrush, Trans. Faraday Soc. 67, 2036 (1971).

7. R. G. Derwent and B. A. Thrush, J. Chem. Soc. Faraday II. 68, 720 (1972).

8. R. G. Derwent and B. A. Thrush, Disc Faraday Soc. 53, 162 (1972).

9. R. G. Aviles, D. F. Muller, and P. L. Houston, Appl. Phys. Lett. 37, 358 (1980).

10. R. F. Heidner III, C. E. Gardner, T. M. El-Sayed, and G. I. Segal, to be published.

11. L. W. Bader and E. A. Ogryzlo, Disc Faraday Soc. 37, 46 (1964).

12. R. F. Heidner and C. E. Gardner, $O_2(^1\Delta)$-I Atom Kinetic Studies, TR-0080(5606)-2, The Aerospace Corporation, El Segundo, California (8 November 1979).

13. D. W. Trainor, D. O. Ham, and F. Kaufman, J. Chem. Phys. 58, 4599 (1972).

14. J. H. Miller, R. W. Boese, and L. P. Giver, J. Quant. Spec. Rad. Transfer 9, 1507 (1969).

15. R. M. Badger, A. C. Wright, and R. F. Whitlock, J. Chem. Phys. 43, 4345 (1965).

16. R. H. Garstang, J. Res. Nat. Bur. Stand. 68, 61 (1964).

17. R. J. O'Brien, Jr. and G. H. Myers, J. Chem. Phys. 53, 3832 (1970).

18. P. M. Borrell, P. Borrell, K. R. Grant, and M. D. Pedley, J. Photochem. 9, 107 (1970).

19. P. Borrell, P. M. Borrell, M. D. Pedley, and K. R. Grant, <u>Proc. Roy. Soc. London A.</u> <u>367</u>, 395 (1979).

20. L. R. Martin, R. B. Cohen, and J. F. Schatz, <u>Chem. Phys. Lett.</u> <u>41</u>, 394 (1976).

21. S. A. Lawton, S. E. Novick, H. P. Broida, and A. V. Phelps, <u>J. Chem. Phys.</u> <u>66</u>, 1381 (1977).

22. P. Borrell, P. M. Borrell, and M. D. Pedley, <u>Chem. Phys. Lett.</u> <u>51</u>, 300 (1977).

23. H. Lilenfeld, private communication, 1980.

24. U. Schurath, <u>J. Photochem.</u> <u>4</u>, 215 (1975).

25. J. I. Steinfeld and D. G. Sutton, <u>Chem. Phys. Lett.</u> <u>64</u>, 550 (1979).

LABORATORY OPERATIONS

The *Laboratory Operations* of The Aerospace Corporation is conducting experimental and theoretical investigations necessary for the evaluation and application of scientific advances to new military concepts and systems. Versatility and flexibility have been developed to a high degree by the laboratory personnel in dealing with the many problems encountered in the nation's rapidly developing space and missile systems. Expertise in the latest scientific developments is vital to the accomplishment of tasks related to these problems. The laboratories that contribute to this research are:

Aerophysics Laboratory: Launch and reentry aerodynamics, heat transfer, reentry physics, chemical kinetics, structural mechanics, flight dynamics, atmospheric pollution, and high-power gas lasers.

Chemistry and Physics Laboratory: Atmospheric reactions and atmospheric optics, chemical reactions in polluted atmospheres, chemical reactions of excited species in rocket plumes, chemical thermodynamics, plasma and laser-induced reactions, laser chemistry, propulsion chemistry, space vacuum and radiation effects on materials, lubrication and surface phenomena, photosensitive materials and sensors, high precision laser ranging, and the application of physics and chemistry to problems of law enforcement and biomedicine.

Electronics Research Laboratory: Electromagnetic theory, devices, and propagation phenomena, including plasma electromagnetics; quantum electronics, lasers, and electro-optics; communication sciences, applied electronics, semiconducting, superconducting, and crystal device physics, optical and acoustical imaging; atmospheric pollution; millimeter wave and far-infrared technology.

Materials Sciences Laboratory: Development of new materials; metal matrix composites and new forms of carbon; test and evaluation of graphite and ceramics in reentry; spacecraft materials and electronic components in nuclear weapons environment; application of fracture mechanics to stress corrosion and fatigue-induced fractures in structural metals.

Space Sciences Laboratory: Atmospheric and ionospheric physics, radiation from the atmosphere, density and composition of the atmosphere, aurorae and airglow; magnetospheric physics, cosmic rays, generation and propagation of plasma waves in the magnetosphere; solar physics, studies of solar magnetic fields; space astronomy, x-ray astronomy; the effects of nuclear explosions, magnetic storms, and solar activity on the earth's atmosphere, ionosphere, and magnetosphere; the effects of optical, electromagnetic, and particulate radiations in space on space systems.

THE AEROSPACE CORPORATION
El Segundo, California

DATE
FILMED

—8